Aust. J. Phys., 1993, **46**, 359–80

Electronic Properties of Quasi-One-Dimensional Semiconductor Nanostructures: Plasmons and Exchange-Correlation Effects in Quantum Wires*

S. Das Sarma and Ben Yu-Kuang Hu

Department of Physics, University of Maryland,
College Park, MD 20742-4111, U.S.A.

Abstract

We review the many-body exchange-correlation properties of electrons confined to the lowest sub-band of a quantum wire, including effects of impurity scattering. Without impurity scattering, the virtual excitations of arbitrarily low energy one-dimensional plasmons destroy the Fermi surface of the electrons, whereas the presence of impurity scattering damps out the low energy plasmons and *restores* the Fermi surface. The electron inelastic scattering rate Γ in the absence of scattering is zero below a critical wavevector k_c corresponding to the plasmon emission threshold, above which Γ diverges as $(k-k_c)^{-1/2}$ for $k \to k_c$. For typical wire widths and electron densities currently available, the calculated bandgap renormalisation is found to be on the order of 10–20 meV. We also calculate the finite-temperature inelastic scattering rates and mean free paths of electrons injected into a quantum wire containing a quasi-one-dimensional electron gas. We show that there is a very sharp increase in the electron scattering rate at the one-dimensional plasmon emission threshold. Based on these results, we suggest the possibility of a one-dimensional hot-electron device which possesses an $I-V$ curve with a sharp onset of a large negative differential resistance. We also present a general method for obtaining expressions for the analytic continuation of finite-temperature self-energies which are suitable for use in numerical computations. In the case of the GW approximation for the self-energy, this method gives the finite-temperature generalisation of the zero-temperature 'line and pole' decomposition. This formalism is used to calculate the finite-temperature self-energy and bandgap renormalisation of electrons in the extreme quantum limit of a quantum wire. A brief review of the experimental and theoretical status of plasmons in quantum wire structures is given.

1. Introduction

In this article we review some of our recent theoretical work (Hu and Das Sarma 1992*a*, 1992*b*, Hu 1993) on electronic properties of one-dimensional semiconductor quantum wire structures, with the emphasis on exchange-correlation and collective effects. The main issue addressed here is why the phenomenology of experiments on electronic properties of quantum wires is so well described by considering quantum wires as normal one-dimensional metals. The subject is of considerable fundamental interest because the theoretical consensus developed over the last forty years seems to indicate that one dimension is completely different from two and three dimensions in the sense that any interaction between the electrons

* Paper presented at the Gordon Godfrey Workshop, University of New South Wales, Sydney, 20–21 July 1992.

0004-9506/93/030359$05.00

leads to the vanishing of the Fermi surface in one dimension and the concepts of quasiparticles and Landau–Fermi liquid theory, which are the central paradigms for higher-dimensional electron systems, do not apply. Thus, the reason why the current experimental situation in quantum wires is consistent with the picture of a normal one-dimensional Fermi liquid is a puzzle requiring understanding.

The rest of this review is organised as follows. In Section 2 we discuss the basic theory of exchange-correlation effects in quantum wires, explaining how impurity disorder effects could, in principle, stabilise the one-dimensional Fermi surface. In Section 3 we describe a proposed nonlinear quantum wire device which utilises special properties of one-dimensional systems. In Section 4 we discuss the finite-temperature exchange-correlation effects, introducing a general many-body technique for calculating finite-temperature self-energies in interacting Fermi systems. We conclude in Section 5 by presenting some results for one-dimensional plasmon dispersion.

2. Exchange-Correlation Effects

There has been a great deal of recent interest (see e.g. Reed and Kirk 1989; Kirk and Reed 1992) in ultranarrow confined semiconductor systems, called quantum wire structures, where electron dynamics is essentially restricted to being one-dimensional. Such quantum wires, with active widths (along the plane of confinement) smaller than 300 Å and of negligible (less than 100 Å) thickness, have recently been fabricated (Plaut *et al.* 1991; Goñi *et al.* 1991), and continued improvement in growth and fabrication techniques should lead to even more confined and better defined wires in the near future. While there is much excitement about the potential applications of these semiconductor quantum wires as high-speed transistors and efficient photodetectors and lasers, these systems have also generated great fundamental physical interest as examples of *real* one-dimensional Fermi gases, where one-dimensional electron dynamics can be studied in a controlled and quantitative manner (just as semiconductor inversion layers, heterojunctions and quantum wells have been serving as useful physical models for two-dimensional Fermi systems for the last decade or so). Recent fabrication breakthroughs have allowed the attainment of the *truly* one-dimensional electric quantum limit, in the sense that only one quantum sub-band is populated by the electrons in the quantum wire, so that the one-dimensional interacting Fermi gas model is valid. Theory predicts very unusual properties for interacting one-dimensional Fermi systems, and the semiconductor quantum wires should be ideal for observing these properties experimentally. However, in all experiments reported thus far (e.g. Plaut *et al.* 1991; Goñi *et al.* 1991; Cingolani *et al.* 1991; Calleja *et al.* 1991) the electronic properties of quantum wires seem to be explicable on the basis of a normal one-dimensional Fermi liquid model.

We have recently investigated (Hu and Das Sarma 1992*a*), within a many-body perturbation theory, why the one-dimensional electrons confined in quantum wires seem to behave as normal Fermi liquids, despite convincing and well accepted theoretical claims that both disorder and interaction effects are singular in one dimension and should lead to ground states which are drastically different from normal Fermi liquids [such as strongly localised systems or Luttinger liquids (Tomonaga 1950; Luttinger 1963; Dzyaloshinskii and Larkin 1973)]. Our calculation is, to the best of our knowledge, the first complete realistic theory of

many-body exchange-correlation effects in one-dimensional quantum wire systems. Similar early calculations (Vinter 1975; Lee *et al.* 1975; Ando 1976; Das Sarma *et al.* 1989) in two-dimensional electron gas systems were useful and important in the development of that subject.

We begin by mentioning three important ways in which an *ideal* one-dimensional electron gas is *theoretically* expected to be *strikingly different* from its higher-dimensional counterparts. In each case, a perturbation to the system, which in higher dimensions tends to leave the system in a Fermi liquid state, theoretically *drastically* changes the behaviour of the system in one dimension (i.e., the Fermi liquid behaviour is a highly unstable fixed point in one dimension). We then argue that *actual* semiconductor quantum wires may behave differently from the theoretical zero-temperature ideal because of the effects of finite-temperature, finite size and scattering, which may serve to stabilise Fermi liquid behaviour in the semiconductor quantum wires.

First, the presence of any electron–phonon coupling (which is invariably present) in a one-dimensional system theoretically should result in a lattice Peierls (1955) distortion accompanied by a charge-density wave ground state at zero temperature. However, in actual semiconductor quantum wires, the electron–phonon interaction via the deformation potential coupling is so weak that even at the low temperatures at which experiments on these systems are performed, the Peierls distortion does not occur. The second important consideration for quantum wires is disorder-induced Anderson (1958) localisation: in one dimension (unlike higher dimensions) the presence of *any* disorder localises all non-interacting electronic states. The currently fabricated semiconductor quantum wires are obviously not disorder-free, and hence in the electric quantum limit all the quantum wire electronic states are exponentially Anderson-localised, and the concept of an electron gas strictly should not apply here. However, we argue that in the state-of-the-art high-quality semiconductor quantum wires, fabricated with the aid of modulation doping techniques, typical localisation lengths are very long (many microns) and therefore in these wires the electrons may be considered to be extended for all experimental purposes. It should, however, be mentioned that Anderson localisation is the property of a non-interacting disordered electron gas and, in the presence of electron–electron interaction, one-dimensional exponentially localised states may be delocalised.

The third important way in which ideal one-dimensional Fermi gases differ from equivalent higher-dimensional systems is that the presence of particle–particle interactions theoretically makes the Fermi liquid model inapplicable to one-dimensional systems. Instead, the paradigm for interacting one-dimensional Fermi systems is the strongly correlated Luttinger (also called Tomonaga–Luttinger) liquid. Hence in the electric quantum limit semiconductor quantum wires should behave as Luttinger liquids. In experiments involving luminesence, inelastic light scattering, far infrared spectroscopy, capacitance studies, etc., on the other hand, quantum wires have shown no obvious sign of Luttinger liquid behaviour, seemingly behaving instead as *normal* one-dimensional Fermi liquids. For instance, an essential feature of a Luttinger liquid is that it has no Fermi surface (i.e. the momentum distribution function n_k is continuous through the Fermi momentum k_F) and yet luminesence experiments show large Fermi edge singularities (Calleja *et al.* 1991). In a recent paper we have suggested, based on the theoretical results

reviewed here, that in real quantum wires, impurity effects can suppress Luttinger liquid behaviour in semiconductor quantum wires, causing them to behave as normal one-dimensional Fermi liquids. Thus the effects of the strong correlations of the Luttinger liquid, like the Peierls instability and Anderson localisation, may be negligible in real quantum wires. The fact that quantum wire experimental results are routinely interpreted on the basis of a one-dimensional normal metal model indicates that these peculiarities must not be strongly present in real systems.

We calculate the zero-temperature leading-order (in the dynamically screened interaction) self-energy $\Sigma(k,\omega)$ of electrons that are confined to the lowest energy sub-band of a quantum wire of width a and zero thickness with infinite potential barriers. We ignore contributions from higher energy sub-bands on the grounds that they should be irrelevant in the limit where the electron Fermi energy is much smaller than the sub-band energy separation. The calculation can be extended to include higher sub-bands. Knowledge of $\Sigma(k,\omega)$ allows one to calculate many experimentally observable one-electron properties of a system. We calculate $\Sigma(k,\omega)$ using the so-called GW approximation (Hedin 1965) which has been highly successful in describing properties of real two- and three-dimensional electron systems. $\Sigma(k,\omega)$ is determined by the dynamical screening properties of the electron gas in the wire, which is quantified by the dielectric function $\epsilon(q,\omega)$. We assume that $\epsilon(q,\omega)$ is given by the random phase approximation (RPA) (Li and Das Sarma 1989, 1991) which has recently been shown (Li *et al.* 1992) to exactly reproduce the plasmon dispersion of one-dimensional systems. We include the effects of impurity scattering on $\epsilon(q,\omega)$ through the modification given by Mermin (1970) in which the scattering is described by a single relaxation rate γ.

A system is a Fermi liquid if it possesses a Fermi surface (i.e. a discontinuity in n_k) whose presence is indicated by a δ-function in the spectral function $A(k,\omega)$ at $k = k_{\mathrm{F}}$ and $\omega = 0$. The existence of a $\delta(\omega)$ in $A(k_{\mathrm{F}},\omega)$ depends crucially on the behaviour of $\mathrm{Im}[\Sigma(k_{\mathrm{F}},\omega)]$ as $\omega \to 0$. If $|\mathrm{Im}[\Sigma(k_{\mathrm{F}},\omega)]|$ goes to zero faster than $|\omega|$, then $A(k_{\mathrm{F}},\omega)$ has a $\delta(\omega)$, indicating that the system is a Fermi liquid. The discontinuity in n_k at k_{F} is proportional to the weight of this δ-function and is called the renormalisation factor Z_{F} (Mahan 1990). In contrast, if $|\mathrm{Im}[\Sigma(k_{\mathrm{F}},\omega)]|$ goes to zero slower than $|\omega|$, then there is *no* δ-function in $A(k_{\mathrm{F}},\omega)$, implying that the system is *not* a Fermi liquid. Two- and three-dimensional systems without disorder are in general Fermi liquids (Luttinger 1961; Chaplik 1971). Through a study of $\mathrm{Im}[\Sigma_{\mathrm{ret}}(k_{\mathrm{F}},\omega)]$ we show that in one dimension the system is (is not) a Fermi liquid in the the presence (absence) of impurity scattering.

The imaginary part of $\Sigma(k_{\mathrm{F}},\omega)$ is a measure of the virtual transition rate to all states of energy less than ω away from the Fermi energy. At low energies in two and three dimensions, single-particle scattering is far more important than plasmon scattering because the single-particle excitation spectrum is gapless and the phase space available for single-particle scattering extends around the entire Fermi surface, whereas the plasmon dispersion either rises quickly or has a gap at $q = 0$. Therefore, for small ω, the major contribution to $\mathrm{Im}[\Sigma(k_{\mathrm{F}},\omega)]$ in two and three dimensions comes from *virtual single-particle excitations*. In contrast, in one dimension, the single-particle excitation spectrum has a gap except at $|q| = 0, 2k_{\mathrm{F}}$, and the phase space available for single-particle scattering is severely

restricted, while the plasmon dispersion is gapless at $q = 0$. Hence, in one dimension, $\mathrm{Im}[\Sigma(k_\mathrm{F},\omega)]$ at small ω is dominated not by virtual single-particle excitations but by the *virtual excitation of plasmons*. This unique feature of one-dimensional systems gives rise to interesting consequences, which we describe next.

In the case of a clean quantum wire ($\gamma = 0$), we find within the RPA that the dominance of the virtual low energy plasmon excitations results in $|\,\mathrm{Im}[\Sigma(k_\mathrm{F},\omega)]\,| \sim |\omega|\,|\ln(|\omega|)|^{\frac{1}{2}}$, indicating, as noted earlier, that the Fermi surface does not exist (in agreement with Luttinger liquid theory). In other words, because of the ease with which particles at the Fermi surface can emit virtual low energy plasmons, the Fermi surface smears out to the extent that a sharp discontinuity in n_k no longer exists. However, the inclusion of impurity scattering causes the electrons to diffuse at long wavelengths, which damps out the plasmons at small q. Hence the plasmon contribution to $\mathrm{Im}[\Sigma(k_\mathrm{F},\omega)]$ at small $|\,\omega|$ is removed, resulting in $|\,\mathrm{Im}[\Sigma(k_\mathrm{F},\omega)]\,| \sim \omega^2|\ln(|\omega|)|^3$ as $|\,\omega| \to 0$, which implies that the Fermi surface is restored. This result indicates that the Fermi surface is resurrected in dirty systems because the low energy virtual plasmon emission responsible for its destruction in clean systems has been suppressed by impurity scattering.

In Fig. 1 we show our calculated Fermi distribution function $n_k = (2\pi)^{-1}\int d\omega\, A(k,\omega)$ for various values of the impurity scattering rate γ. We emphasise that γ was included only in the dynamical screening function and *not* in the single-electron Green's function because we wanted to determine whether the suppression of the emission of low energy virtual plasmons produces a discontinuity in n_k. Figure 1 clearly shows a discontinuity in n_k at $k = k_\mathrm{F}$ for $\gamma/E_\mathrm{F} \neq 0$. Note that if we had included effects of γ (or finite temperature) in the single-electron Green's function, n_k would have been broadened in the usual way and the result would look very similar to non-singular higher-dimensional broadened Fermi functions. In the inset to Fig. 1 we show the calculated Z_F as a function of the impurity scattering rate. For $\gamma = 0$, $Z_\mathrm{F} = 0$, indicating that there is no Fermi surface, but as scattering is increased Z_F also increases until it saturates at very large γ (where our results should not be trusted because our treatment ignores localisation). Note that Z_F goes to zero slowly as $\gamma \to 0$, implying that even a small amount of impurity scattering results in a fairly pronounced discontinuity in n_k at k_F.

Figure 2 shows the inelastic scattering rates of quasiparticles in the conduction band $\Gamma(k) = 2|\,\mathrm{Im}[\Sigma(k,\omega = \xi_k)]\,|$, where ξ_k is the electron energy relative to the chemical potential, for parameters corresponding to $a = 100$ Å and a density of $n = 0{\cdot}56 \times 10^6\ \mathrm{cm}^{-1}$ in GaAs. For $\gamma = 0$, below a threshold wavevector k_c, there is *no* electron–electron scattering (within the RPA) because in a strictly one-dimensional system, conservation of energy and momentum restricts electron–electron scattering to an exchange of particles, which is not a randomising process because electrons are indistinguishable. (Our treatment ignores multiparticle excitations, which will give rise to a nonzero scattering rate for $k < k_\mathrm{c}$.) For $k > k_\mathrm{c}$, a new scattering channel opens in which electrons genuinely emit plasmons (as opposed to the virtual plasmon excitations at the Fermi surface). The inelastic scattering rate diverges as $\sim(k - k_\mathrm{c})^{-1/2}$ as one approaches k_c from above, due to the divergence in the density of states available for scattering

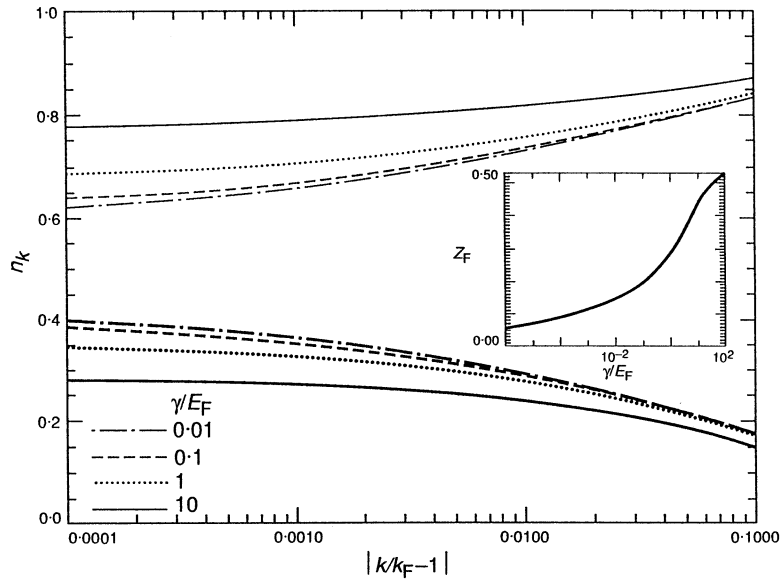

Fig. 1. Momentum distribution function n_k of a quasi-one-dimensional electron gas around $k/k_F = 1$, for various impurity scattering rates γ. The parameters used are $k_F a = 0{\cdot}9$ and $r_s = (2m_e e^2/\pi\hbar^2 k_F \kappa) = 0{\cdot}7$, which for GaAs correspond to $a = 100$ Å and density of $0{\cdot}56 \times 10^6\,\mathrm{cm}^{-1}$, giving a Fermi energy $E_F = 4{\cdot}4$ meV $= 50$ K $= (\hbar\times)\,6{\cdot}7 \times 10^{12}\,\mathrm{s}^{-1}$ and an average Coulomb potential energy between electrons of $2e^2 k_F/\pi\kappa = 6{\cdot}2$ meV. The bold lines refer to $k > k_F$, and the thin lines to $k < k_F$. For $\gamma = 0$, n_k is continuous at $k = k_F$, implying that the system is a non-Fermi liquid, but for $\gamma \neq 0$ a discontinuity occurs at $k = k_F$, signalling the presence of a Fermi surface. The inset shows the Fermi surface renormalisation factor Z_F, which gives the magnitude of the discontinuity in n_{k_F}, as a function of γ.

right at the plasmon emission threshold. For $\gamma \neq 0$, the inelastic scattering rate remains finite because the plasmon line is broadened. Furthermore, the breaking of translational invariance relaxes momentum conservation, permitting inelastic scattering via single-particle excitations for $k < k_c$. The inset in Fig. 2 shows the inelastic mean free path, $l = v(k)/\Gamma(k)$, where v is the electron velocity.

In Fig. 3 we show the results of the calculation of the the bandgap renormalisation (the sum of $\mathrm{Re}[\Sigma(k = 0, \omega = \xi_{k=0})]$ of conduction band electrons and valence band holes) due to the presence of the conduction electrons. These results should be useful in explaining photoluminescence experiments in quantum wires, even though we only have electrons in our calculation whereas the experiments contain both electrons and holes, because we expect the holes to have a negligible effect on the bandgap renormalisation due to their large mass (and hence their inability to screen effectively).

Finally, we discuss differences between our model and the Luttinger model, on which the properties of the Luttinger liquid are based. We assume a finite density of electrons in a parabolic energy dispersion, whereas the Luttinger model assumes

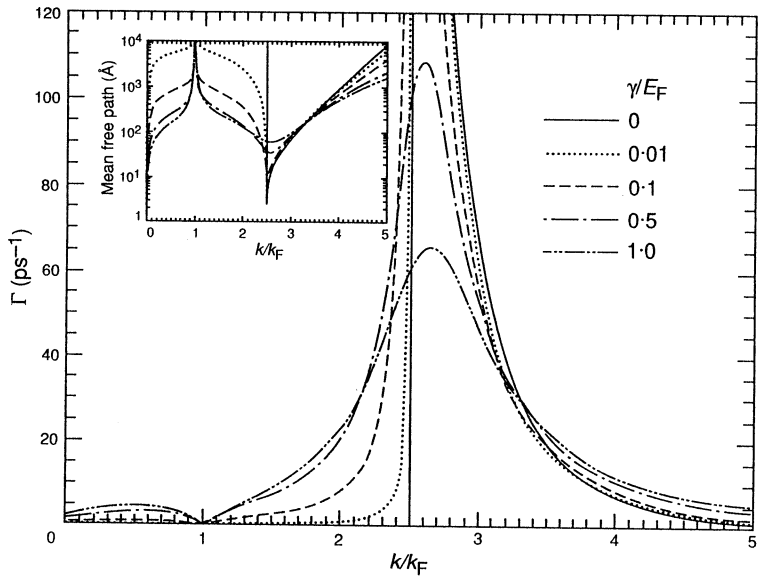

Fig. 2. Inelastic scattering rates $\Gamma(k)$, as a function of k, for various electron impurity scattering rates γ, for $k_F a = 0{\cdot}9$ and $r_s = 0{\cdot}7$. Within the RPA, for $\gamma = 0$, $\Gamma(k)$ is identically zero below $k = k_c$ because energy and momentum conservation prohibits single particle excitations and plasmon emissions. Above k_c the scattering rate is caused by plasmon emissions. For $\gamma \neq 0$ the plasmon line broadens and momentum conservation is relaxed, resulting in a nonzero Γ for $k < k_c$. The inset shows the corresponding mean free path $l(k) = \Gamma(k)k/m$.

an *infinite* density of negative energy electrons in a completely linear dispersion. We use the *actual* Coulomb interaction (Das Sarma and Lai 1985) between electrons for a rectangular well [a reasonably realistic model for confinement (Laux *et al.* 1988)], whereas the Luttinger model assumes an unrealistic short-range potential. On the other hand, we carry out the self-energy calculation only to leading order in the dynamically screened interaction, whereas the solution of the Luttinger model includes all vertex corrections and is exact. Thus, ours is a leading-order calculation of a realistic model, whereas the Luttinger model is an exact result to an unrealistic model.

3. Device Applications

Based on the results reviewed in Section 2, we proposed (Hu and Das Sarma 1992*b*) a novel device principle which directly uses the many-body properties of a one-dimensional quantum Fermi liquid. We show here that it may be possible to obtain a device with a large and sudden onset of negative differential resistance (NDR) (i.e. $dI/dV < 0$). This sudden onset of NDR could be exploited to produce a transistor, while the NDR itself suggests that this device might be used as an oscillator (e.g. in analogy with the Gunn oscillator or, more recently,

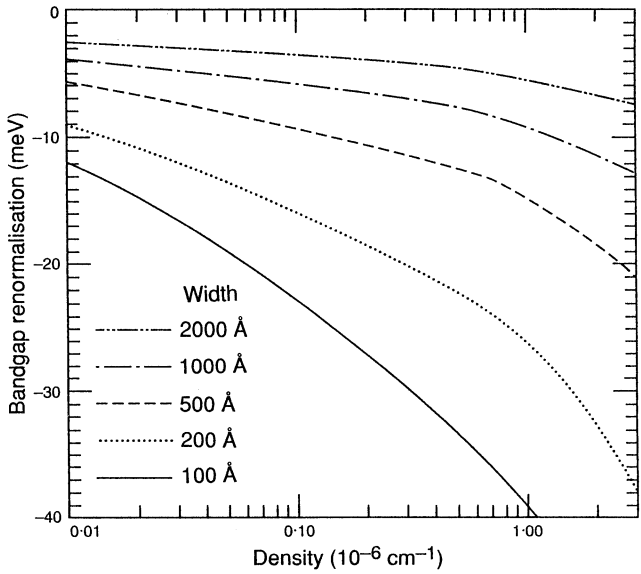

Fig. 3. Total bandgap renormalisation ($\mathrm{Re}[\Sigma_e + \Sigma_h]$ at $k = 0$, $\omega = \xi_{k=0}$) as a function of electron density in the quantum wire, for various wire widths with parameters corresponding to GaAs.

the resonant tunnelling diode). In the proposed device principle, the predicted NDR is associated with a *sharp* change in the inelastic mean free path of the injected electrons at a specific energy: in the ideal system at $T = 0$, the mean free path changes from being infinite below the threshold voltage to being zero above it.

The device principle which we propose may be experimentally observed in the quasi-one-dimensional version of the tunnelling hot electron transistor amplifier (THETA), shown schematically in Fig. 4, which has been fabricated successfully in three and two dimensions (Levi *et al.* 1985; Heiblum *et al.* 1985; Sivan *et al.* 1989). We assume that the quasi-one-dimensional device is in the extreme quantum limit, i.e. that all the electrons are in the lowest energy sub-band in the device. Electrons are injected from an emitter at energies above the Fermi energy E_F into a base region which contains (either through doping or electrostatic confinement) a one-dimensional electron gas, and the injected electrons that travel through the base region enter the collector on the opposite side of the base. The fraction of electrons that reach the collector depends on the mean free path (and hence the scattering rate) of the injected electrons, and the mean free path is in general a strong function of the momentum $\hbar k$ (or equivalently, the energy) of the injected electrons and the electron density in the base region.

In two and three dimensions, the main scattering mechanism for these electrons in the THETA devices is provided by the coupled plasmon–optic-phonon modes (Jalabert and Das Sarma 1989). However, in the semiconductor quantum wires

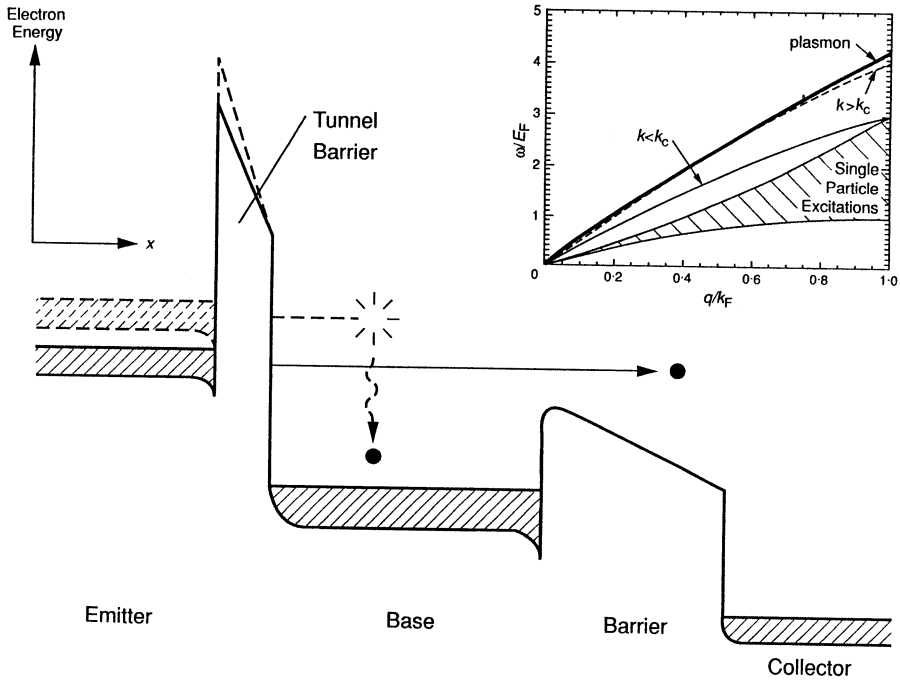

Fig. 4. A schematic of the band diagram of a one-dimensional tunnelling hot electron transistor, where electrons are injected from the emitter into the base (which contains a Fermi sea of electrons) with some fraction of the injected electrons reaching the collector. The solid (dashed) line indicates injection of the electrons into the base region below (above) the plasmon emission threshold (i.e., the solid line is for $k < k_c$ and the dashed line is for $k > k_c$). The inset shows the energy versus momentum-loss diagram for the injected electron. The intersections of the energy versus momentum-loss curve and the plasmon dispersion curve (bold line) indicates the wavevectors at which plasmons are emitted; if there is no intersection (as with the solid line), plasmon emissions are not allowed. As the energy of the injected electrons is raised above the plasmon emission threshold, the scattering rate increases dramatically (see Fig. 5), drastically reducing the fraction of injected electrons that reach the collector.

in the extreme quantum limit that are currently being fabricated, the densities of the electrons in the base are low enough that all the energy scales associated with the electron gas and operation of the device (E_F, plasmon energy and electron injection energy) are much smaller than the optic phonon energy, and therefore the optic phonons play a negligible rôle. Acoustic phonons can also be ignored because they couple very weakly to electrons in III–V semiconductors, and the associated scattering rates are on the order of $10^{10}\,s^{-1}$. We assume that impurity scattering in the wires is negligible, which is not unreasonable given the excellent and continually improving techniques for fabricating these mesoscopic systems. This last assumption is equivalent to assuming that the *elastic* mean free paths are much longer than the inelastic mean free path to be calculated in this paper—given that our calculated inelastic mean free paths are generally a few thousand Å or less, and that in good quality quantum wires

elastic mean free paths are many microns, the neglect of impurity scattering is a good approximation for our purposes. Thus the main scattering mechanism for an injected electron is the interaction with the electron gas in the base.

As emphasised in Section 2, in strictly one-dimensional systems with a parabolic band, the only pair electron–electron scattering (where the injected electron scatters with a single particle in the base) allowed by conservation of energy and momentum is an exchange of particles, which is not a randomising process because the electrons are indistinguishable. Multi-particle scattering (interactions of the injected electron involving two or more other electrons) is of higher order in the screened interaction, and therefore we ignore it because we expect its contribution to be small. The only scattering mechanism left that is responsible for preventing the injected electrons from reaching the collector is the interaction of the injected electrons with the plasmons (i.e. collective density oscillations) of the electron gas in the base, which we review in the last section.

Not all injected electrons can emit plasmons. Because the plasmon dispersion in quasi-one-dimensional systems goes as (Das Sarma and Lai 1985) $\omega(q) \sim q|\ln(qa)|^{\frac{1}{2}}$, where a is the width of the wire, only injected electrons with large enough kinetic energies can emit plasmons (see inset to Fig. 4). At $T = 0$, for a given density n, there is therefore a threshold wavevector $k_c(n)$ below which no plasmon emission can take place. Within the approximations we have used and at $T = 0$, as k is increased through k_c, the scattering rate jumps from *zero* to *infinity* (equivalently, the mean free path falls from *infinity* to *zero*); this divergence in the scattering rate at $k = k_c$ is due to phase space features that are peculiar to one-dimensional systems. This result indicates that as the bias voltage is increased so that the k of the injected electrons rises above k_c (or equivalently if n is decreased so that k_c falls below k), the jump in the scattering rate should be spectacular, and the current passing from emitter to collector should fall dramatically. Thermal and impurity effects will broaden the divergence in the scattering rate, but, as we show below, this effect persists up to relatively high temperatures.

Using the Born approximation, we calculate the finite-temperature momentum (or transport) scattering rate, $\Gamma_{t,k}$, which is the quantity that is relevant to the decay in current.* The momentum scattering rate at temperature T is given by the integral over wavevectors of the scattering probabilities, weighted by the change in momentum, i.e. (see e.g. Pines and Nozières 1966)

$$\Gamma_{t,k} = 2\int_{-\infty}^{\infty} dq\,\frac{q}{k}\,V_c(q)\,\mathrm{Im}\left[\epsilon^{-1}(q,\omega_k(q))\right]\frac{1}{1-\exp[\omega_k(q)/k_BT]} \times [1 - f_{eq}(k+q)]\,. \tag{1}$$

Here $\omega_k(q) = E(k+q) - E(k)$ [where $E(k) = \hbar^2k^2/2m$ is the electron kinetic energy], $V_c(q)$ is the Coulomb matrix element for electrons in the lowest sub-band

* The total finite-temperature Born approximation scattering rate is actually *infinite* due to the divergence in the factor $[1 - \exp(\omega_k(q)/k_BT)]^{-1}$ at small q. However, these small-q scattering events have little effect on the degradation of the current, which is the quantity of interest here. Therefore, we calculate the more physically meaningful quantity $\Gamma_{t,k}$.

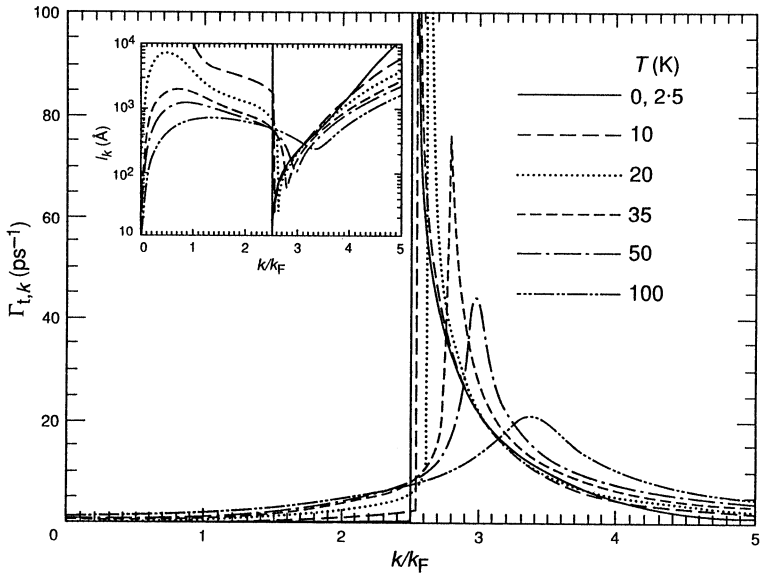

Fig. 5. Momentum scattering rate $\Gamma_{t,k}$ of an electron in a doped one-dimensional quantum wire, as a function of electron momentum for various temperatures. The parameters used are $k_F a = 0{\cdot}9$ (k_F is the Fermi wavevector) and $r_s = (2m_e e^2/\pi\hbar^2 k_F \kappa) = 0{\cdot}7$. The insets show the corresponding mean free path, $l_k = v_k/\Gamma_{t,k}$.

of a square quantum well of width a with hard walls, $f_{eq}(k)$ is the Fermi–Dirac distribution at temperature T, and $\epsilon(q,\omega)$ is the dielectric function of the one-dimensional electron gas, within the random phase approximation (RPA).

In Fig. 5 we show the results of our calculation of $\Gamma_{t,k}$, and the corresponding mean free path, $l_k = v_k/\Gamma_{t,k}$ (where $v_k = \hbar k/m$ is the electron velocity). In the case of $T = 0$, the Born-approximation $\Gamma_{t,k}$ is exactly zero up to the plasmon emission threshold, and it diverges as $(k-k_c)^{-1/2}$ as $k \to k_c^+$. As the temperature is increased, the divergence becomes a finite peak due to the broadening of the plasmon line through Landau damping, and the peak shifts to higher energies. The shift of the peak is due to an upward shift in energy of the plasmon dispersion curve with increasing temperature, which is a well known phenomenon in plasma physics. In one dimension, the plasmon dispersion for small q is

$$\omega^2(q) \approx \frac{nq^2 V_c(q)}{m}\left(1 + \frac{3m\langle v^2\rangle}{nV_c(q)}\right), \tag{2}$$

where $\langle v^2\rangle$ denotes the average of v^2 over the distribution of the electron gas in the base. For a one-dimensional Fermi gas, to order T^2,

$$\langle v^2\rangle = \frac{v_F^2}{3}\left[1 + \frac{\pi^2}{4}\left(\frac{k_B T}{E_F}\right)^2\right], \tag{3}$$

explicitly showing the upward shift in the plasmon dispersion with increasing temperature. The sharp drop in the mean free path persists to relatively high temperatures (here on the order of tens of degrees for the parameters chosen), and therefore should be experimentally observable. We believe that this sharp drop in the inelastic mean free path will produce a large NDR in quantum wires as the injected electrons pass through the threshold energy.

We note that the RPA *exactly* reproduces the collective mode spectrum for the exactly soluble Luttinger model for one-dimensional systems (Li *et al.* 1992). Since our results are mainly based on this collective mode behaviour, the RPA should be a good approximation for our purposes.

We have shown in this section that, due to the sudden onset of a very large $\Gamma_{t,k}$ caused by the emission of plasmons in a doped quasi-one-dimensional quantum wire, a one-dimensional THETA device could show an $I-V$ curve with a sudden onset of large negative differential resistance. This characteristic could have applications in switching devices or oscillators. Note that in higher-dimensional electron systems there is a plasmon threshold as well where the onset of plasmon emission occurs. The effect in higher dimensions, however, is not dramatic because the ideal mean free path does not change from being infinite below the threshold to zero above (as it does in the one-dimensional system), since single-particle scattering contributes in higher dimensions, in contrast to the situation in one dimension. Thus, our proposed NDR in quantum wires is a specific one-dimensional many-body property.

4. Finite Temperature Results

Powerful field-theoretic techniques, including Feynman diagram perturbation methods, were developed several decades ago as a tool for calculating physical properties of interacting quantum systems. First to be introduced was the zero-temperature formalism, which allowed the ground state properties of an interacting system to be calculated. Subsequently, Matsubara (1955) introduced a similar formalism for finite-temperature systems, which was formally identical to the zero-temperature formalism. The zero-temperature formalism has generally been used for many-body quasiparticle calculations for metals because the energy scales intrinsic to the problem (Fermi energy, plasmon energy, etc.) are usually much larger than the temperature T. However, in semiconductors, especially in artificial structures of reduced dimensionality, because of the low electron densities and large dielectric constants involved, the experimental temperature can be comparable to the intrinsic energy scales of the electron gas. In these cases, the zero-temperature formalism may not provide an adequate description of the system, and therefore the finite-temperature formalism is needed.

While the finite-temperature formalism is easier to handle than the zero-temperature formalism in some ways, using it involves an extra hurdle. With the finite-temperature formalism, one obtains an expression for the electron self-energy $\sigma(i\nu_n)$ that is only valid at discrete points $i\nu_n \equiv i(2n+1)\pi T$ on the complex frequency plane, where n is an integer. (In this paper, we set $\hbar = k_B = 1$.) The $\sigma(i\nu_n)$ must be *analytically continued* to the complex plane to obtain the self-energy $\Sigma(z)$ that is valid for all complex frequencies from which the retarded self-energy, the quantity relevant to experiments, can be obtained by setting $z = \omega + i0^+$. (In this paper we use the convention that functions denoted by

upper case characters are analytic in the frequency variable while those denoted by lower case characters may be non-analytic.)

In principle, one can obtain from $\sigma(i\nu_n)$ a formal expression for $\Sigma(z)$ in terms of integrals over spectral representations, but the expressions for $\Sigma(z)$ obtained in this manner involve integration over one or more frequency variables, which makes them inefficient for use in numerical computations. On previous occasions various approximations, such as the plasmon-pole approximation, were used to obtain the finite-temperature self-energy (Das Sarma *et al.* 1979; Das Sarma and Vinter 1982). In this paper we present a more direct method of analytically continuing the $\sigma(i\nu_n)$ to $\Sigma(z)$, which yields an exact expression that is much more amenable to numerical calculation.

In a nutshell, the method uses the properties which the analytic continuation of $\sigma(i\nu_n)$ must satisfy to lead us to its analytic continuation, $\Sigma(z)$. These properties are as follows: (i) $\Sigma(z)$ is analytic on the entire complex frequency plane, with the exception of branch cuts on the real axis (henceforth, when we say a function is 'analytic' it is with the implicit understanding that it could have branch cuts on the real axis); (ii) $\Sigma(z{=}i\nu_n) = \sigma(i\nu_n)$ for all $i\nu_n$; and (iii) $\Sigma(z)$ goes to a constant as $|z| \to \infty$. These properties ensure a unique analytic continuation (Baym and Mermin 1961). By systematically fulfilling each of the above conditions, we are led directly to the desired analytic continuation.

We elucidate this method by examining a simple example, that of the self-energy within the GW approximation see Fig. 6*a* of a translationally invariant system. The self-energy can be written as a sum of a frequency-independent exchange and a frequency-dependent correlation part, $\sigma(\mathbf{k}, i\nu_n) = \sigma_{\rm ex}(\mathbf{k}) + \sigma_{\rm cor}(\mathbf{k}, i\nu_n)$. The exchange part, which is frequency-independent (and hence already analytic), is given by $\sigma_{\rm ex}(\mathbf{k}) = -(2\pi)^{-d} \int \mathrm{d}\mathbf{q}\; V_{\rm c}(\mathbf{q})\; n_{\rm F}(\xi_{\mathbf{k}+\mathbf{q}})$, where $V_{\rm c}(\mathbf{q})$ is the bare Coulomb interaction, $n_{\rm F}(x) = [\exp(x/T) + 1]^{-1}$ is the Fermi function, $\xi_{\mathbf{k}+\mathbf{q}}$ is the kinetic energy relative to the chemical potential and d is the dimension of the system. The $\sigma_{\rm cor}(\mathbf{k}, i\nu_n)$ is given by

$$\sigma_{\rm cor}(\mathbf{k}, i\nu_n) = -\int \frac{\mathrm{d}\mathbf{q}}{(2\pi)^d}\; h_{\mathbf{k},\mathbf{q}}(i\nu_n)\,, \tag{4}$$

where

$$h_{\mathbf{k},\mathbf{q}}(i\nu_n) = T\sum_{i\omega_n} \frac{w(\mathbf{q}, i\nu_n)}{i\nu_n + i\omega_n - \xi_{\mathbf{k}+\mathbf{q}}}\,. \tag{5}$$

Here the frequency summation is over the boson frequencies $i\omega_n = i2\pi nT$ (n are integers), and $w(\mathbf{q}, i\nu_n) = V_{\rm c}(\mathbf{q})[\epsilon^{-1}(\mathbf{q}, i\nu_n) - 1]$ is the difference between the screened and bare Coulomb interactions. The problem is to analytically continue $\sigma_{\rm cor}(\mathbf{k}, i\nu_n)$ to $\Sigma_{\rm cor}(\mathbf{k}, z)$.

From (4), finding an analytic continuation $\Sigma_{\rm cor}(\mathbf{k}, z)$ of $\sigma_{\rm cor}(\mathbf{k}, i\nu_n)$ is equivalent to finding the analytic continuation $H_{\mathbf{k},\mathbf{q}}(z)$ of $h_{\mathbf{k},\mathbf{q}}(i\nu_n)$. Thus if we construct a function $H_{\mathbf{k},\mathbf{q}}(z)$ such that (I) it is analytic (in the sense mentioned above), and (II) $H_{\mathbf{k},\mathbf{q}}(z{=}i\nu_n) = h_{\mathbf{k},\mathbf{q}}(i\nu_n)$, then

$$\Sigma_{\rm cor}(\mathbf{k}, z) = -\int \frac{\mathrm{d}\mathbf{q}}{(2\pi)^d} H_{\mathbf{k},\mathbf{q}}(z) \tag{6}$$

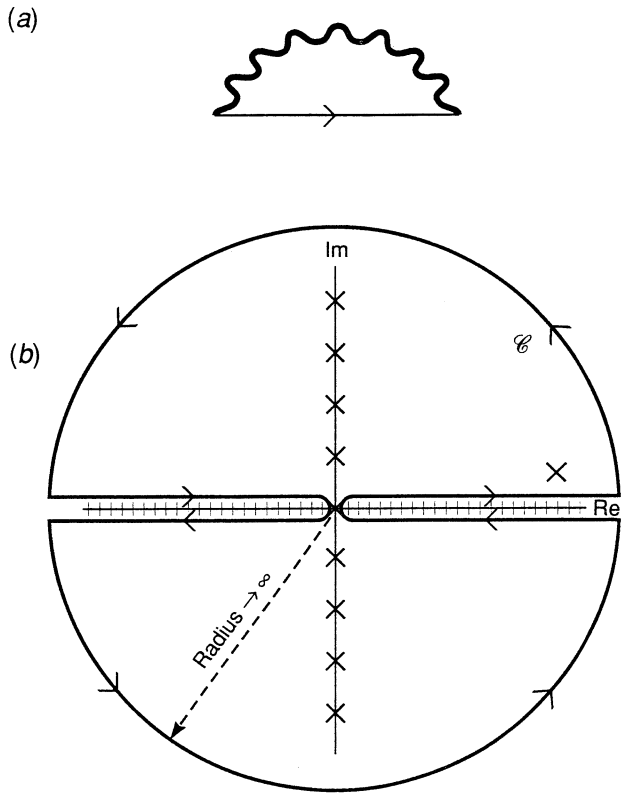

Fig. 6. (*a*) The diagram for the GW approximation to the self-energy. The thick wavy line indicates the screened Coulomb interaction, while the straight solid line is the bare-electron Green function. (*b*) The contour of integration C for (7). The hatched real axis indicates a branch cut due to $w(\mathbf{q},\omega)$ in the integrand of (7). The crosses mark the poles due to the integrand; the ones on the imaginary axis are due to $n_{\mathrm{B}}(\omega)$, and the isolated pole is due to the denominator. The residues of the poles on the imaginary axis give $h_{\mathbf{k},\mathbf{q}}(z)$, while the residue of the isolated pole gives $\tilde{h}_{\mathbf{k},\mathbf{q}}(z)$.

automatically satisfies the conditions (i) and (ii) above. Note that the simple replacement $i\nu_n \rightarrow z$ in (5) gives a function $h_{\mathbf{k},\mathbf{q}}(z)$ that has poles at $z = \xi_{\mathbf{k}+\mathbf{q}} - i\omega_n$ for all n and thus, because it violates condition (I), is not the desired analytic continuation $H_{\mathbf{k},\mathbf{q}}(z)$.

The outline of the procedure for obtaining the function $H_{\mathbf{k},\mathbf{q}}(z)$ which satisfies conditions (I) and (II) is as follows. First, we write down a function $H^{\mathrm{A}}_{\mathbf{k},\mathbf{q}}(z) = h_{\mathbf{k},\mathbf{q}}(z) + \tilde{h}_{\mathbf{k},\mathbf{q}}(z)$, where $\tilde{h}_{\mathbf{k},\mathbf{q}}(z)$ is chosen so that it *cancels* all the singularities in $h_{\mathbf{k},\mathbf{q}}(z)$ on the complex plane. Thus $H^{\mathrm{A}}_{\mathbf{k},\mathbf{q}}(z)$ is *analytic*, fulfilling condition (I). However, $\tilde{h}_{\mathbf{k},\mathbf{q}}(z)$ is in general nonzero at $z = i\nu_n$, and hence $H^{\mathrm{A}}_{\mathbf{k},\mathbf{q}}(i\nu_n) \neq h_{\mathbf{k},\mathbf{q}}(i\nu_n)$, violating condition (II). The second step is therefore to add an additional analytic term $H'_{\mathbf{k},\mathbf{q}}(z)$ which *cancels* $\tilde{h}_{\mathbf{k},\mathbf{q}}(z)$ at all $z = i\nu_n$. Since the function $H^{\mathrm{A}}_{\mathbf{k},\mathbf{q}}(z) + H'_{\mathbf{k},\mathbf{q}}(z)$ is analytic *and* equals $h_{\mathbf{k},\mathbf{q}}(z)$ for all $z = i\nu_n$,

fulfilling both conditions (I) and (II), it is the desired analytic continuation $H_{\mathbf{k},\mathbf{q}}(z)$. With this $H_{\mathbf{k},\mathbf{q}}(z)$, $\Sigma_{\rm cor}(\mathbf{k},z)$ given by (6) satisfies conditions (i) and (ii) above. Condition (iii) can be checked at the end; in the case of the GW approximation (and in other cases we have studied) it is satisfied.

In the case of the GW self-energy, $H^{\rm A}_{\mathbf{k},\mathbf{q}}(z)$ is given by

$$H^{\rm A}_{\mathbf{k},\mathbf{q}}(z) = \int_{\mathcal{C}} \frac{{\rm d}\omega}{2\pi i} \frac{w(\mathbf{q},\omega)\, n_{\rm B}(\omega)}{z+\omega-\xi_{\mathbf{k}+\mathbf{q}}}\,, \tag{7}$$

where $n_{\rm B}(\omega) = [\exp(\omega/T)-1]^{-1}$ is the Bose distribution function, and the contour of integration $\mathcal{C}$ is shown in Fig. 6*b*. The function $H^{\rm A}_{\mathbf{k},\mathbf{q}}(z)$ is clearly analytic (off the real axis) in the variable z. By the residue theorem, $H^{\rm A}_{\mathbf{k},\mathbf{q}}(z)$ is given by the sum of the residues of the poles from $n_{\rm B}(\omega)$ and the denominator in the integrand of (7) [note that $w(\mathbf{q},\omega)$ is analytic everywhere except for a branch cut on the real axis], yielding

$$H^{\rm A}_{\mathbf{k},\mathbf{q}}(z) = h_{\mathbf{k},\mathbf{q}}(z) + \tilde{h}_{\mathbf{k},\mathbf{q}}(z)\,, \tag{8}$$

where

$$h_{\mathbf{k},\mathbf{q}}(z) = T\sum_{i\omega_n} \frac{w(\mathbf{q},i\omega_n)}{z+i\omega_n-\xi_{\mathbf{k}+\mathbf{q}}},$$

$$\tilde{h}_{\mathbf{k},\mathbf{q}}(z) = w(\mathbf{q},\xi_{\mathbf{k}+\mathbf{q}}-z)\; n_{\rm B}(\xi_{\mathbf{k}+\mathbf{q}}-z). \tag{9}$$

Despite being the sum of two nonanalytic functions, $H^{\rm A}_{\mathbf{k},\mathbf{q}}(z)$ is analytic because the poles that occur at $z=\xi_{\mathbf{k}+\mathbf{q}}-i\omega_n$ for $h_{\mathbf{k},\mathbf{q}}(z)$ are exactly cancelled by the the poles in $\tilde{h}_{\mathbf{k},\mathbf{q}}(z)$.* However, because $\tilde{h}_{\mathbf{k},\mathbf{q}}(i\nu_n)\neq 0$, $H^{\rm A}_{\mathbf{k},\mathbf{q}}(z)$ does not fulfil condition (II). In order to fulfil condition (II), we need to add an analytic function which cancels $\tilde{h}_{\mathbf{k},\mathbf{q}}(z)$ at $z=i\nu_n$.

Since $i\nu_n = i(2n+1)\pi T$, for all integers n, $n_{\rm B}(\xi_{\mathbf{k}+\mathbf{q}}-i\nu_n)\equiv -n_{\rm F}(\xi_{\mathbf{k}+\mathbf{q}})$, and thus $\tilde{h}_{\mathbf{k},\mathbf{q}}(i\nu_n) = -w(\mathbf{q},\xi_{\mathbf{k}+\mathbf{q}}-i\nu_n)\, n_{\rm F}(\xi_{\mathbf{k}+\mathbf{q}})$. Therefore the analytic term needed to cancel $\tilde{h}_{\mathbf{k},\mathbf{q}}(i\nu_n)$ is

$$H'_{\mathbf{k},\mathbf{q}}(z) = w(\mathbf{q},\xi_{\mathbf{k}+\mathbf{q}}-z)\, n_{\rm F}(\xi_{\mathbf{k}+\mathbf{q}})\,. \tag{10}$$

Hence, $H_{\mathbf{k},\mathbf{q}}(z) = H^{\rm A}_{\mathbf{k},\mathbf{q}}(z) + H'_{\mathbf{k},\mathbf{q}}(z)$ is given by (8), (9) and (10), and the correlation self-energy in the GW approximation is, from (6),

$$\begin{aligned}\Sigma_{\rm cor}(\mathbf{k},z) &= -\int \frac{{\rm d}\mathbf{q}}{(2\pi)^d}\; [H^{\rm A}_{\mathbf{k},\mathbf{q}}(z) + H'_{\mathbf{k},\mathbf{q}}(z)] \\ &= -\int \frac{{\rm d}\mathbf{q}}{(2\pi)^d}\, T\sum_{i\omega_n} \frac{w(\mathbf{q},i\omega_n)}{z+i\omega_n-\xi_{\mathbf{k}+\mathbf{q}}} \\ &\quad -\int \frac{{\rm d}\mathbf{q}}{(2\pi)^d}\, w(\mathbf{q},\xi_{\mathbf{k}+\mathbf{q}}-z)[n_{\rm B}(\xi_{\mathbf{k}+\mathbf{q}}-z)+n_{\rm F}(\xi_{\mathbf{k}+\mathbf{q}})]\,. \end{aligned} \tag{11}$$

* Recall that the Bose function can be written as $n_{\rm B}(\zeta) = -\frac{1}{2} + T\sum_{i\omega_n}(\zeta-i\omega_n)^{-1}$.

The retarded self-energy, $\Sigma_{\rm ret}(\mathbf{k},\omega)$, is obtained by setting $z \to \omega + i0^+$. The first and second terms on the right-hand side of (11) are, respectively, the finite-temperature generalisation of the so-called 'line' and 'pole' components of the GW approximation of the $T = 0$ correlation self-energy (Quinn and Ferrell 1958). As in the zero-temperature case, the line contribution is completely real because $w(\mathbf{q}, -i\omega_n)$ and $w(\mathbf{q}, i\omega_n)$ are complex conjugates, and hence the total contribution to the imaginary part of $\Sigma_{\rm ret}(\mathbf{k},\omega)$ comes from the pole part.

As in the $T = 0$ case, in the GW approximation the 'on-shell' imaginary part of the self-energy, $|\,\mathrm{Im}[\Sigma_{\rm ret}(\mathbf{k},\omega{=}\xi_{\mathbf{k}})]\,|$, is half the sum of the Born-approximation electron and hole scattering rates. Using the identity

$$n_{\rm B}(\xi_{\mathbf{k+q}} - \omega) + n_{\rm F}(\xi_{\mathbf{k+q}}) = n_{\rm B}(\xi_{\mathbf{k+q}} - \omega)[1 - n_{\rm F}(\xi_{\mathbf{k+q}})] - n_{\rm B}(\omega - \xi_{\mathbf{k+q}}) n_{\rm F}(\xi_{\mathbf{k+q}})\,, \tag{12}$$

we can write $2\,|\mathrm{Im}[\Sigma_{\rm ret}(\mathbf{k},\xi_{\mathbf{k}})]\,| = \gamma_{\rm e}(\mathbf{k}) + \gamma_{\rm h}(\mathbf{k})$, where

$$\gamma_{\rm e}(\mathbf{k}) = -\int \frac{\mathrm{d}\mathbf{q}}{(2\pi)^d}\; 2\,V_{\rm c}(\mathbf{q})\,\mathrm{Im}[\epsilon^{-1}(\mathbf{q},\xi_{\mathbf{k+q}} - \xi_{\mathbf{k}})] n_{\rm B}(\xi_{\mathbf{k+q}} - \xi_{\mathbf{k}})[1 - n_{\rm F}(\xi_{\mathbf{k+q}})]\,,$$

$$\gamma_{\rm h}(\mathbf{k}) = \int \frac{\mathrm{d}\mathbf{q}}{(2\pi)^d}\; 2\,V_{\rm c}(\mathbf{q})\,\mathrm{Im}[\epsilon^{-1}(\mathbf{q},\xi_{\mathbf{k+q}} - \xi_{\mathbf{k}})] n_{\rm B}(\xi_{\mathbf{k}} - \xi_{\mathbf{k+q}})\, n_{\rm F}(\xi_{\mathbf{k+q}}) \tag{13}$$

are the Born-approximation electron and hole scattering rates respectively.

The method outlined above can also be used for higher-order diagrams. The procedure is analogous to the one carried out above, i.e. one first obtains an analytic function $H^{\rm A}_{\mathbf{k},\mathbf{q}}(z) = h_{\mathbf{k},\mathbf{q}}(z) + \tilde{h}_{\mathbf{k},\mathbf{q}}(z)$ by writing $H^{\rm A}_{\mathbf{k},\mathbf{q}}(z)$ in terms of integrals of the form (7). One finds the analytic $H'_{\mathbf{k},\mathbf{q}}(z)$ necessary to cancel out the $\tilde{h}_{\mathbf{k},\mathbf{q}}(z)$ at $z = i\nu_n$. The number of terms needed to obtain $H_{\mathbf{k},\mathbf{q}}(z)$ increases somewhat from the example given above [for the second-order term for the self-energy with two screened Coulomb interactions, six terms are needed in addition to $h_{\mathbf{k},\mathbf{q}}(z)$], but writing $\Sigma_{\rm ret}(\mathbf{k},z)$ in the manner prescribed above generally reduces integrals over spectral representations to sums over complex frequencies, which aids numerical computation. Note that this technique is independent of system dimensionality and can be used in higher dimensions as well.

Because the energy scales of the electron gas in semiconductor quantum wire structures are small (e.g. Fermi energies of 5 meV $\sim$ 50 K), even small temperatures may affect their many-body properties significantly. We therefore apply (11) to the calculation of the self-energy and bandgap renormalisation of electrons in a one-dimensional quantum wire in the extreme quantum limit (i.e. assuming that the electrons only occupy the lowest energy sub-band). We use the RPA form for the dielectric function $\epsilon(q,z)$, which we evaluate numerically using an expression given by Maldague (Maldague 1978; Das Sarma 1986).

In Fig. 7 we show the real and imaginary parts of the retarded self-energy of a quantum wire (with a parabolic band in the unconfined direction) as a function of frequency for $k = 0$. The discontinuities in $\mathrm{Im}[\Sigma_{\rm ret}(\omega)]$ at $T = 0$, which arise from virtual plasmon emission thresholds, broaden with increasing

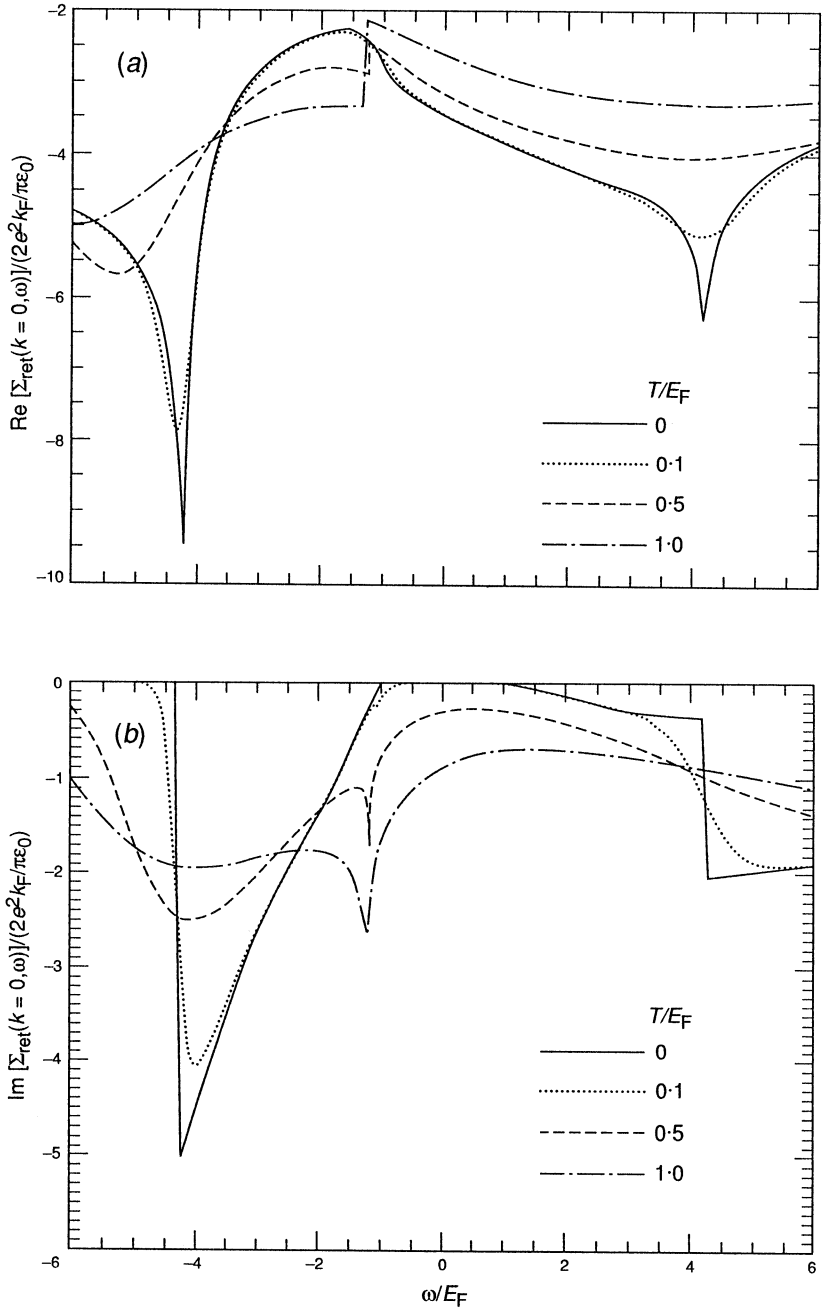

Fig. 7. Real (a) and imaginary (b) parts of the $k = 0$ self-energy (in the GW approximation, where W is screened interaction given by the random phase approximation) as a function of frequency for a quasi-one-dimensional electron gas, at various temperatures. As in Fig. 5, parameters used here are $k_F a = 0{\cdot}9$ and $r_s = 0{\cdot}7$. A logarithmic divergence develops at $\omega = \xi_k$ (the 'on-shell' frequency) in $\mathrm{Im}\Sigma_{\mathrm{ret}}(k,\omega)$ for $T \neq 0$ because the Born approximation electron–electron scattering rate at $T \neq 0$ in a one-dimensional electron gas is infinite.

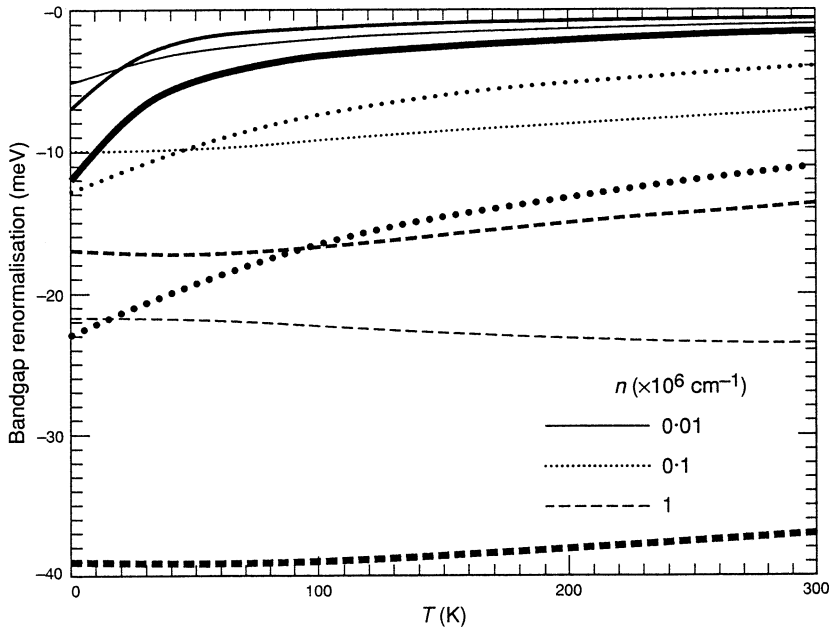

Fig. 8. Bandgap renormalisation due to conduction electrons as a function of temperature, for a wire width of 100 Å in GaAs, for various electron densities: The thin line is for the electrons ($\mathrm{Re}[\Sigma_{\mathrm{electron}}(k{=}0, \xi_{k=0})]$), the light bold line is for the holes ($\mathrm{Re}[\Sigma_{\mathrm{hole}}(k{=}0, \xi_{k=0})]$), and the heavy bold line is for the sum of the two. The densities $n = 0{\cdot}01 \times 10^6$ cm^{-1}, $0{\cdot}1 \times 10^6$ cm^{-1} and 1×10^6 cm^{-1} correspond to Fermi temperatures of $E_{\mathrm{F}} = 1{\cdot}6 \times 10^{-2}$ K, 1·6 K and 160 K, respectively.

temperature because the plasmon peaks are broadened by Landau damping. The logarithmic divergence in the imaginary part of the self-energy which develops at $\omega = \xi_k$ when T is increased from zero is unique to one-dimensional systems: in $d = 1$ at $\omega = \xi_k$, there is a non-integrable q^{-1} singularity in the integrand in (11), corresponding to a divergence in the Born-approximation electron–electron scattering at small momentum transfer. (In higher dimensions this singularity is removed by the phase space factor q^{d-1}.) Concomitant with the divergence in $\mathrm{Im}[\Sigma_{\mathrm{ret}}(k, \xi_k)]$ is a discontinuity in $\mathrm{Re}[\Sigma_{\mathrm{ret}}(k, \xi_k)]$, since the real and imaginary parts are related by the Kramers–Kronig relations.

In Fig. 8 we show the electron and hole bandgap renormalisation due to the presence of conduction electrons. These results are relevant to photoluminescence experiments in GaAs, even though the calculation ignores the screening effects of holes, because the holes are ineffective at screening due to their heavy mass. Due to the discontinuity in $\mathrm{Re}[\Sigma_{\mathrm{ret}}(k, \xi_k)]$, we take $\frac{1}{2}\,\mathrm{Re}[\Sigma_{\mathrm{ret}}(k, \xi_k + 0^+) + \Sigma_{\mathrm{ret}}(k, \xi_k - 0^+)]$ at $k = 0$ to be the bandgap renormalisation. We find that for very low densities, where the Fermi temperature is low, the bandgap renormalisation can change by approximately an order of magnitude when the temperature increases from $T = 0$ to $T = 300$ K.

5. Plasmons

In this section we provide a brief review of the RPA theory of one-dimensional plasmons, which have recently been observed (Goñi *et al.* 1991) via Raman scattering spectroscopy in GaAs quantum wires. It is worth while to note that the recent experimental measurement of one-dimensional plasmon dispersion in GaAs quantum wires is in excellent quantitative agreement with the earlier simple RPA predictions of Das Sarma and Lai (1985) and Li and Das Sarma (1989, 1991) showing the RPA to be a valid description of plasmons in one dimension, somewhat in contrast with one's intuitive expectation that it should be a poor approximation in lower dimensions.

Within the RPA, the plasmon dispersion is given by (Pines and Nozières 1966) the vanishing of the dielectric function $\epsilon(q,\omega) = 1 - V_c(q)\,\Pi_0(q,\omega)$, where $V_c(q)$ is the Coulomb interaction and Π_0 is the non-interacting, dynamical irreducible polarisability. The long-wavelength plasmon frequency, ω_p, in d dimensions is easily obtained by noting that

$$\Pi_0(q,\omega) = \frac{nq^2}{m\omega^2} \tag{14}$$

and

$$V_c(q) \sim \begin{cases} q^{1-d}, & \text{if } d = 2,3, \\ |\ln(qa)|, & \text{if } d = 1, \end{cases} \tag{15}$$

which gives $\omega_p \sim$ constant, $q^{\frac{1}{2}}$ and $q\,|\ln(qa)|^{\frac{1}{2}}$ in $d = 3, 2, 1$ dimensions respectively. The length a, introduced essentially as an infrared cutoff in $d = 1$, is the width of the quantum wire. We mention that the plasmon is massless or ungapped in both $d = 1$ and $d = 2$ (i.e. $\omega_p \to 0$ as $q \to 0$) due to the fact that in lower dimensions there is no long-range electrostatic restoring force for sinusoidal charge perturbations. Of course in $d = 3$, the plasmon mode has a finite long-wavelength frequency given by $\omega_p = [4\pi ne^2/(\kappa m)]^{\frac{1}{2}}$, where κ is the background dielectric constant, arising from the long range nature of the restoring forces in the three-dimensional Coulomb interaction.

The full dispersion for one-dimensional plasmons is obtained by using the analytical result for $\Pi_0(q,\omega)$ (Li and Das Sarma 1989)

$$\Pi_0(q,\omega) = \frac{m}{\pi q} \ln \left| \frac{\omega^2 - \omega_-^2(q)}{\omega^2 - \omega_+^2(q)} \right|, \tag{16}$$

where $\omega_\pm(q) = qv_F \pm q^2/(2m)$. The RPA equation $\epsilon(q,\omega_p) = 1 - V_c(q)\Pi(q,\omega_p) = 0$ is now easily solved to give the following one-dimensional plasmon dispersion relation

$$\omega_p(q) = A(q)\left[\frac{\omega_+^2(q) - \omega_-^2(q)}{A(q) - 1}\right]^{\frac{1}{2}}, \tag{17}$$

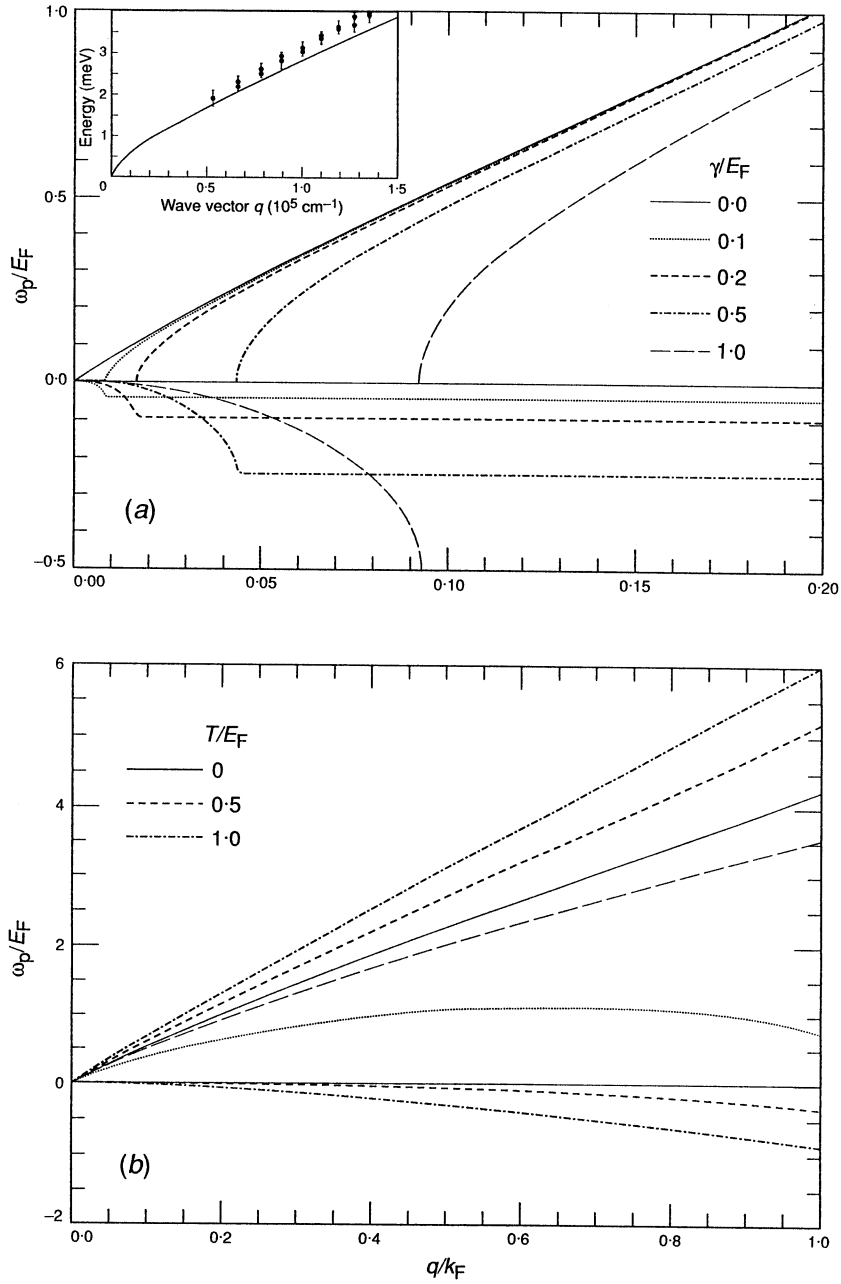

Fig. 9. Calculated one-dimensional plasmon dispersion in a GaAs quantum wire within the RPA for (*a*) $T = 0$ and various values of γ, (*b*) $\gamma = 0$ and various temperatures, calculated by finding the zeros of $\epsilon(q,\omega)$ on the complex frequency plane. The curves with $\omega > 0$ give the real part and those with $\omega < 0$ give the imaginary part. The curves include full $V_c(q)$ for infinite square-well confinement. As in previous figures, the system parameters are $k_F a = 0{\cdot}9$ and $r_s = 0{\cdot}7$, which, for GaAs, correspond to a Fermi wavevector of $k_F = 0{\cdot}88 \times 10^6$ cm^{-1}. In (*b*) we show both the long-wavelength result, $\omega_p^2 = nq^2 V_c(q)/m$, using $V_c(q) = 2e^2|\ln(qa)|/\kappa$ (dash–triple-dot line), and the full $V_c(q)$ (long-dashed lines). Experimental results of Goñi *et al.* (1991) compared with RPA theory Li *et al.* (1992) are shown as an inset in Fig. 9*a*.

where $A(q) = \exp[q\pi/mV_c(q)]$. An expansion (Li *et al.* 1992) to second order in q/k_F gives

$$\omega_p(q) = |q| \left[v_F^2 + \frac{2}{\pi} v_F V_c(q) \right]^{\frac{1}{2}} + O(q^3), \tag{18}$$

which is exactly the same dispersion relation as that for the low-lying collective mode (see e.g. Mahan 1990) in the Tomonaga–Luttinger liquid. Thus the RPA and Tomonaga–Luttinger collective mode dispersions are the same in one dimension, explaining why the experimental results (Goñi *et al.* 1991) for one-dimensional plasmon dispersion agree so well with the RPA theory.

It is easy to show (Das Sarma and Lai 1985) that, in one dimension, $V_c(q \to 0) \sim |\ln(qa)|$ for any reasonable confinement model and, therefore, $\omega_p \sim |q|\,|\ln(qa)|^{\frac{1}{2}}$ in $d = 1$ as discussed above. In Fig. 9 we show some numerical results for one-dimensional plasmon dispersion including quantum finite-size effects, finite-temperature effects, and finite-level-broadening effects. The quantum finite-size effect is included in the theory by calculating $V_c(q)$ for the lowest one-dimensional sub-band within the infinite square-well confinement model. Finite-temperature effects are included by calculating (Maldague 1978; Das Sarma 1986) $\Pi_0(q, \omega)$ at $T \neq 0$, whereas finite-level-broadening effects are included in the Mermin (1970) relaxation-time approximation essentially through the replacement $\omega^2 \to \omega(\omega + i\gamma)$ in Π_0. The plasmon dispersion is obtained by numerically solving $\epsilon(q, \omega_p(q)) = 0$ on the complex frequency plane. Note that the $\epsilon(q, \omega)$ must be *analytically continued* from the upper half to the lower half of the complex plane.

Impurity scattering causes electrons to diffuse. Since $\omega_p(q)$ goes to zero as $q \to 0$ in $d = 1$, the diffusive nature of the electrons causes the plasmons to become *overdamped* at small q, as in $d = 2$ (Giuliani and Quinn 1984). Thus there is a critical wavevector below which plasmon modes cease to exist. At finite temperature, on the other hand, the plasmon modes at low q remain undamped, whereas Landau damping occurs at higher q. This is because Landau damping affects modes, phase velocities on the order of or less than the thermal or Fermi velocity (whichever is larger). At small q, the plasmon phase velocity $\omega_p/q \sim |\ln(qa)| \to \infty$, and hence Landau damping is negligible. As q increases, the phase velocity of the plasmon decreases and hence Landau damping increases. More details on one-dimensional plasmons can be found in Hu and Das Sarma (1993).

Acknowledgements

This work is supported by the U.S. Army Research Office, the Office of Naval Research and the National Science Foundation.

References

Anderson, P. W. (1958). *Phys. Rev.* **109**, 1492.
Ando, T. (1976). *Phys. Rev. Lett.* **36**, 1383.
Baym, G., and Mermin, N. D. (1961). *J. Math. Phys.* **2**, 232.
Calleja, J. M., Goñi, A. R., Dennis, B. S., Weiner, J. S., Pinczuk, A., Schmidtt-Rink, S., Pfeiffer, L. N., West, K. W., Müller, J. R., and Ruckenstein, A. E. (1991). *Solid State Comm.* **79**, 911.

Chaplik, A. V. (1971). *Zh. Eksp. Theor. Fiz.* **60**, 1845 [*Sov. Phys. JETP* **33**, 97].
Cingolani, R., Lage, H., Tapfer, L., Kalt, H., Heitmann, D., and Ploog, K. (1991). *Phys. Rev. Lett.* **67**, 891.
Das Sarma, S. (1986). *Phys. Rev.* B **33**, 5401.
Das Sarma, S., Jalabert, R., and Yang, S. R. (1989). *Phys. Rev.* B **39**, 5516.
Das Sarma, S., Kalia, R. K., Nakayama, M., and Quinn, J. J. (1979). *Phys. Rev.* B **19**, 6397.
Das Sarma, S., and Lai, W.-Y. (1985). *Phys. Rev.* B **32**, 1401.
Das Sarma, S., and Vinter, B. (1982). *Phys. Rev.* B **26**, 960.
Dzyaloshinskii, I. E., and Larkin, A. I. (1973). *Zh. Eksp. Teor. Fiz.* **65**, 411 [*Sov. Phys. JETP* **38**, 202 (1974)].
Giuliani, G. F., and Quinn, J. J. (1984). *Phys. Rev.* B **29**, 1312.
Goñi, A. R., Wiener, J. S., Calleja, J. M., Dennis, B. S., Pfeiffer, L. N., and West, K. W. (1991). *Phys. Rev. Lett.* **67**, 3298.
Hedin, L. (1965). *Phys. Rev.* **139**, A796.
Heiblum, M., Nathan, M. I., Thomas, D. C., and Knoedler, C. M. (1985). *Phys. Rev. Lett.* **55**, 2200.
Hu, B. Y.-K. (1993). *Phys. Rev.* B **47**, 1687.
Hu, B. Y.-K., and Das Sarma, S. (1992*a*). *Phys. Rev. Lett.* **68**, 1750.
Hu, B. Y.-K., and Das Sarma, S. (1992*b*). *Appl. Phys. Lett.* **61**, 1208.
Hu, B. Y.-K., and Das Sarma, S. (1993). *Phys. Rev.* B (in press).
Jalabert, R., and Das Sarma, S. (1989). *Phys. Rev.* B **40**, 9723.
Kirk, W. P., and Reed, M. A. (Eds) (1992). 'Nanostructures and Mesoscopic Systems' (Academic: Boston).
Laux, S., Frank, D., and Stern, F. (1988). *Surf. Sci.* **196**, 101.
Lee, T. K., Ting, C. S., and Quinn, J. J. (1975). *Phys. Rev. Lett.* **35**, 1048.
Levi, A. F. J., Hayes, J. R., Platzman, P. M., and Wiegmann, W. (1985). *Phys. Rev. Lett.* **55**, 2071.
Li, Q., and Das Sarma, S. (1989). *Phys. Rev.* B **40**, 5860.
Li, Q. P., and Das Sarma, S. (1991). *Phys. Rev.* B **43**, 11768.
Li, Q. P., Das Sarma, S., and Joynt, R. J. (1992). *Phys. Rev.* B **45**, 13713.
Luttinger, J. M. (1961). *Phys. Rev.* **121**, 942.
Luttinger, J. M. (1963). *J. Math. Phys.* **4**, 1154.
Mahan, G. D. (1990). 'Many Particle Physics', 2nd edn (Plenum: New York).
Maldague, P. F. (1978). *Surf. Sci.* **73**, 296.
Matsubara, T. (1955). *Prog. Theor. Phys. (Kyoto)* **14**, 351.
Mermin, N. D. (1970). *Phys. Rev.* B **1**, 2362.
Peierls, R. E. (1955). 'Quantum Theory of Solids' (Clarendon Press: Oxford).
Pines, D., and Nozières, P. (1966). 'The Theory of Quantum Liquids' (W. A. Benjamin: New York).
Plaut, A. S., Lage, H., Grambow, P., Heitman, D., von Klitzing, K., and Ploog, K. (1991). *Phys. Rev. Lett.* **67**, 1642.
Quinn, J. J., and Ferrell, R. A. (1958). *Phys. Rev.* **112**, 812.
Reed, M. A., and Kirk, W. P. (Eds) (1989). 'Nanostructure Physics and Fabrication' (Academic: Boston).
Sivan, U., Heiblum, M., and Umbach, C. P. (1989). *Phys. Rev. Lett.* **63**, 992.
Tomonaga, S. (1950). *Prog. Theor. Phys. (Kyoto)* **5**, 544.
Vinter, B. (1975). *Phys. Rev. Lett.* **35**, 1044.

Manuscript received 17 September 1992, accepted 29 January 1993